

Multi-stepwise GMR and layers magnetic reversal in uniaxial Fe/Cr superlattices

V. V. Ustinov^{*1}, M. A. Milyaev¹, L. N. Romashev¹, T. P. Krinitsina¹, A. M. Burkhanov¹, V. V. Lauter-Pasyuk², and H. J. Lauter¹

¹ Institute of Metal Physics, UD RAS, S. Kavalevskaya Str.18, Ekaterinburg 620041, Russia

² Institute Laue Langevin, BP 56, 38042, Grenoble Cedex 9, France

Received 5 July 2005, revised 17 March 2006, accepted 22 March 2006

Published online 13 April 2006

PACS 75.30.Kz, 75.70.-i, 75.75.+a

We investigated the structure, magnetic and magnetoresistive properties of the antiferromagnetically coupled superlattices $[\text{Fe}(85\text{\AA})/\text{Cr}(t,\text{\AA})]_{12}$ with the Cr layers thickness $t_{\text{Cr}}=12.4$ and 13.6 Å grown simultaneously on (100)MgO and (211)MgO substrates. It is shown that (211)MgO substrate is appropriate for the growth of (210)Fe/Cr multilayers with a strong uniaxial in-plane anisotropy. The stepwise behavior of magnetization and magnetoresistance is revealed in the case when the magnetic field is applied along the easy axis in the film plane of the (211)MgO/[(210)Fe/Cr]₁₂ superlattices. The steps on the $M(H)$ and $\Delta R(H)/R$ dependences are caused by the flip of magnetic moments of individual Fe layers. The qualitative information about the sequence of spin-flip transitions is extracted from the comparative analysis of magnetization and magnetoresistance data.

© 2006 WILEY-VCH Verlag GmbH & Co. KGaA, Weinheim

1 Introduction

It was established recently [1–5] that the magnetic structure of Co-Pt-Ru and Fe-Au multilayers with out-of-plane anisotropy could exist as a set of collinear magnetic states. In such multilayers the transitions between these magnetic states occur as a spin-flip (or meta-magnetic) phase transitions. At that one or several magnetic sublayers reverse their magnetization in narrow intervals of the magnetic field applied along the easy axis. Magnetization reversal processes in the materials result in the appearance of stepped anomalies on a magnetization curve detected mainly by MOKE measurements and sometimes by SQUID/VSM magnetometry [1–3, 6]. The stepped magnetic field dependences of both magnetization and magnetoresistance were investigated in Co-Pd-Ru multilayers [6]. The domain structure of Fe-Au multilayers was studied by the polar magneto-optical Kerr effect [5]. The typical domain sizes were found to be within 10–100 microns in the system. According to the investigation of Hellwig et al. [1–3] the uniform magnetic states exist in macroscopic samples of the Co-Pt-Ru multilayers.

In the paper Rößler and Bogdanov [7] (as well as in [3]) it is pointed out that the unusual reorientation and multidomain effects revealed, for example, in [1–3], are unknown both in bulk magnetics and in easy-plane antiferromagnetic (AF) superlattices. At the same time there are no physical restrictions forbidding the similar reorientation effects in multilayers with in-plane anisotropy. In order to prepare a multilayer with stepped magnetization it is necessary: i) to create in a multilayer the strong uniaxial in-plane anisotropy, the energy of which is comparable or stronger than interlayer exchange coupling, and ii) to apply the magnetic field along the easy axis in the film plane.

In many multilayers consisting of ferromagnetic (FM) and nonmagnetic metals (Fe/Cr, Co/Cu, Co/Ru, etc.) the strength of the exchange coupling and the value of the in-plane anisotropy energy depend on

* Corresponding author: e-mail: ustinov@imp.uran.ru

thickness of nonmagnetic and FM layers, respectively [8–10]. It means that it is possible to find the appropriate combination of layers thickness of magnetic and nonmagnetic materials, and to grow, for example, Fe/Cr multilayer with strong uniaxial in-plane anisotropy.

The two types of MgO substrates are used most often for the growth of Fe/Cr multilayers with in-plane anisotropy, (100)MgO and (110)MgO. The first of them is used for the growth of AF-coupled multilayers with four-fold anisotropy in the film plane. The second one is well known substrate for the growth of (211)Fe/Cr superlattices [11], in which the surface spin-flop transition was observed [12], and also for the synthesis of double superlattice structures with the so called “bias-effect” [13–16]. According to their results the (211)Fe/Cr multilayers have the uniaxial (two-fold) in-plane anisotropy.

However, our attempts to grow by MBE the (211)Fe/Cr superlattices with single-crystal structure were unsuccessful. The transmission electron microscopy (TEM) and tunnel microscopy studies have shown that our (110)MgO/[Fe/Cr]_n multilayers exhibit the parquet-like structure with two types of elongated crystallites. According to the magnetic measurements the samples have four-fold anisotropy with two easy axes canted by the angle of less than 90°. Magnetization curves of these multilayers are smooth when the magnetic field is directed both along easy and hard axes in the film plane. The details of the investigation of (211)Fe/Cr multilayers grown on (110)MgO substrates will be published elsewhere because no spin-flip transitions were detected in these samples. Thus, it was necessary to select other substrate for preparation of Fe/Cr multilayers with strong uniaxial in-plane anisotropy. The substrate is found to be (211)MgO.

The main goals of the present study are the following: i) to demonstrate the appropriateness of (211)MgO substrates for growth of Fe/Cr superlattices with strong uniaxial in-plane anisotropy, ii) to investigate the structure, magnetic and magnetoresistive properties of Fe/Cr superlattices grown on (211)MgO substrates, and iii) to study the peculiarities of multiple spin-flip transitions in these samples.

2 Experiment

The superlattices [Fe(85 Å)/Cr(*t*, Å)]₁₂ consisting of twelve pairs of relatively thick Fe layers and Cr layers with the thickness $t_{Cr} = 12.4$ and 13.6 Å were MBE-grown on (100)MgO and (211)MgO substrates with the Cr(80 Å) buffer layer. The typical deposition rate of Fe and Cr layers was about 1.5 Å/min. The substrate temperature during the buffer layer deposition was $T_{sub} = 300$ °C, whereas at the multilayer growth it was $T_{sub} = 180$ °C. The thicknesses of Fe and Cr layers were chosen to create the uniaxial in-plane anisotropy energy, which could be comparable or stronger than the interlayer exchange coupling. The structures were characterized by TEM and X-ray diffraction. The standard X-ray diffractometer DRON-3M with Co K α radiation and Si-monochromator on the incident beam were used for the low-angle X-ray spectra measurements. The in-plane anisotropy and magnetization curves were studied at room temperature by vibration sample magnetometer with the 360° sample rotation probe. Magnetic properties at low temperatures were measured by superconducting quantum interference device (SQUID) magnetometry. Magnetoresistance was studied by the standard four-probe technique (PPMS, Quantum Design). The sample pieces of 1.5×8 mm and 5×5 mm were used for transport and magnetic measurements, respectively.

3 Results and discussion

Figure 1 shows the low-angle spectra for [Fe(85 Å)/Cr(13.6 Å)]₁₂ superlattices simultaneously grown on (100)MgO and (211)MgO substrates. The coincidence of positions of Bragg reflections is an evidence of the equal superstructure period $L = (t_{Fe} + t_{Cr})$ in these two samples. On the right side of Bragg peaks the additional peaks corresponding to the buffer layer reflections are visible. The amplitude of Kiessig fringes between Bragg peaks is much higher for the superlattice grown on (100)MgO substrate (spectrum (a)) than that for the superlattice grown on (211)MgO substrate (spectrum (b)). It means that interface roughness is bigger in the (211)MgO/Cr(80)/[Fe(85 Å)/Cr(13.6 Å)]₁₂ superlattice (sample 1) in comparison with the (100)MgO/Cr(80)/[Fe(85 Å)/Cr(13.6 Å)]₁₂ superlattice (sample 2).

Figure 2 shows the electron diffraction pattern (EDP) of the sample 1. The EPD includes reflections from both MgO substrate and Fe/Cr multilayer. According to the standard identification procedure [17], these reflections correspond to (211)MgO and (210)Fe/Cr planes. The TEM study has shown that the Fe/Cr multilayer is a pseudo-single-crystal with the preferable orientation (210)Fe/Cr. The epitaxial orientations in this sample are $[100]\text{Fe/Cr} \parallel [110]\text{MgO}$ and $[210]\text{Fe/Cr} \parallel [11\bar{1}]\text{MgO}$. The lattice constants for MgO and Fe/Cr are 4.21 Å and 2.87 Å, respectively. The distance between the nearest atoms in MgO (fcc structure) in the $[11\bar{1}]$ direction is $\sqrt{3} a_{\text{MgO}} = 7.30$ Å, whereas the distance between the nearest atoms in the parallel direction of $[210]\text{Fe/Cr}$ (bcc structure) is $\sqrt{5} a_{\text{Fe}} = 6.41$ Å. The lattice mismatch of $[210]\text{Fe/Cr}$ with $[11\bar{1}]\text{MgO}$ is about 12 %. The similar calculation for $[100]\text{Fe/Cr}$ gives the 3.7 % lattice mismatch with $[110]\text{MgO}$. Thus, the nearest atoms form the rectangle with the sizes of 2.87 Å and 6.41 Å in the (210)Fe plane. The crystal symmetry in the (210)Fe layers causes apparently the uniaxial in-plane anisotropy revealed in the sample (see the insert in Fig. 4). According to magnetic measurements the easy axis is directed along $[100]\text{Fe/Cr}$, whereas the hard axis is directed along $[210]\text{Fe/Cr}$.

Large lattice mismatch (12%) for the $[210]\text{Fe/Cr}$ direction, obviously, stimulates internal strains, which usually relax during a multilayer growth when the total film thickness increases. Due to the strains relaxation the anisotropy constant could be different in Fe layers, which have the nominal equal thickness. Therefore Fe layers could be nonequivalent in the multilayer stack. The interface roughness could

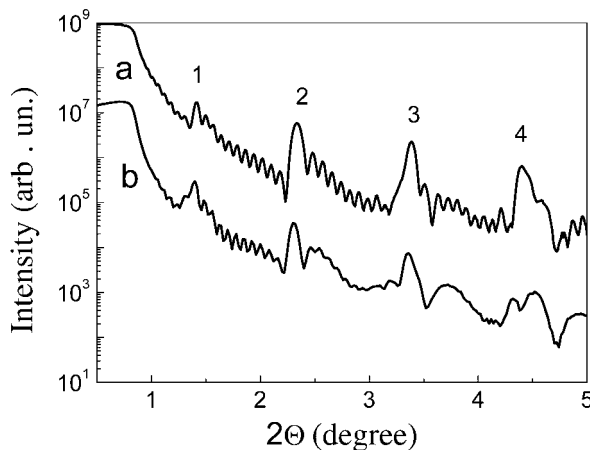


Fig. 1 Low-angle spectra for the sample 2 (a) and the sample 1 (b). The spectrum (a) is shifted upwards by a factor of 100. Bragg reflections are indexed as shown on the spectrum (a).

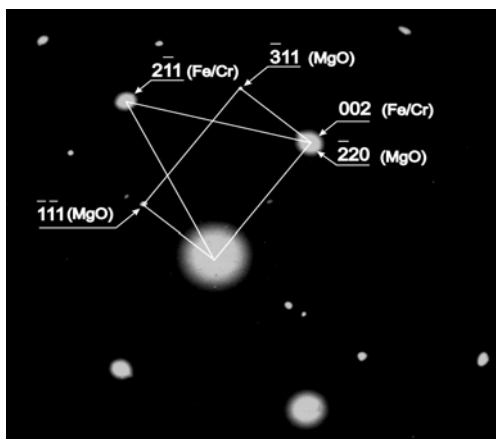


Fig. 2 Electron diffraction pattern for the sample 1. The identified reflections from MgO substrate and Fe/Cr superlattice are presented as shown.

also depend on index of magnetic layers. The growth induced reduction of the interface roughness was discussed by Willekens et al. [6] for the interpretation of the stepped hysteresis loops in Co-Pd-Ru multilayers.

The thicknesses of Cr and Fe layers in our superlattices were chosen on the base of the well-known properties of Fe/Cr multilayers [8–10]. The Cr layer thickness $t_{Cr} \approx 9\div 10$ Å corresponds to the strong antiferromagnetic interlayer coupling, whereas $t_{Cr} \approx 18\div 20$ Å corresponds to the ferromagnetic coupling. The exchange coupling in the $t_{Cr} = 12\div 14$ Å superlattices is still antiferromagnetic one but it is “weak” (the constant of the bilinear exchange coupling is nearly zero in the $t_{Cr} = 14$ Å superlattice). The in-plane anisotropy energy is known to be proportional to the thickness of Fe layers, while the saturation field has the inverse dependence on the Fe layer thickness. We have increased the Fe layer thickness up to $t_{Fe} = 85$ Å. Due to that ($t_{Cr} = 12.4, 13.6$ Å, and $t_{Fe} = 85$ Å) it became possible to reduce the saturation fields H_s of our samples up to the range $|H| < 1$ kOe, where the uniaxial in-plane anisotropy plays important role in the formation of collinear magnetic states.

Fig. 3 shows the magnetoresistance of the sample 1. One can see a number of stepped anomalies on the $\Delta R(H)/R_s$ dependence in the range of magnetic field $|H| \leq 600$ Oe. The shape of the GMR hysteresis loop and the number of stepped anomalies were found to be non-sensitive to the temperature in the range of 2–300 K. The GMR amplitudes in the sample measured at $T = 2$ K and $T = 300$ K are equal to 18 % and 2.4 %, respectively, what is much higher than in Co-Pd-Ru system [6].

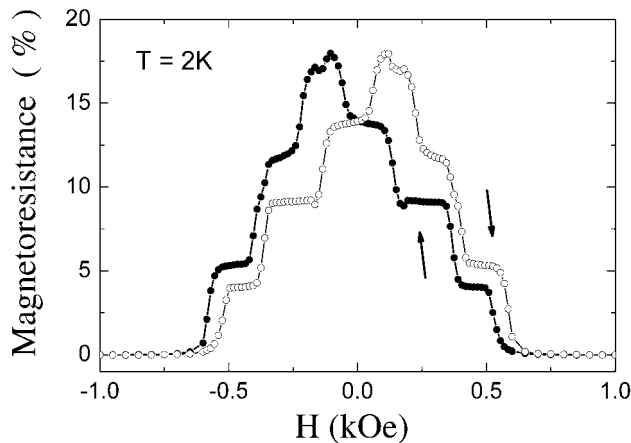


Fig. 3 Magnetoresistance $\Delta R/R_s = [R(H) - R_s]/R_s$ for the sample 1. Magnetic field is applied along the easy axis in the film plane. The R_s is the resistance in the saturation field H_s . The open circles correspond to the ascending branch, and close circles to the descending branch of the GMR hysteresis loop.

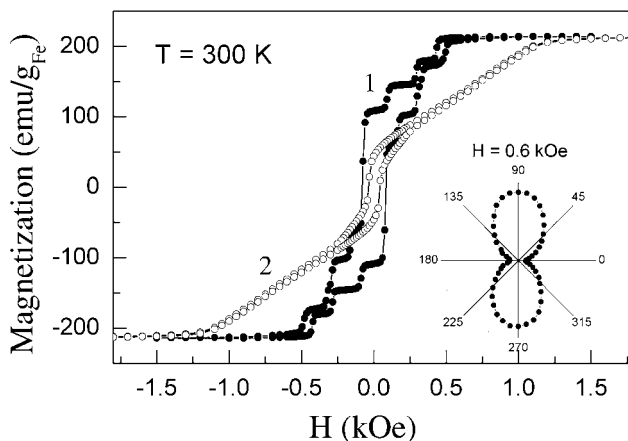


Fig. 4 Magnetization hysteresis loops for the sample 1. The magnetic field is applied along the easy axis (curve 1) and the hard axis (curve 2) in the film plane. The insert demonstrates how the value of the magnetization changes when the sample is rotated in the field $H = 0.6$ kOe around the normal to the surface. Magnetic field is applied in the film plane.

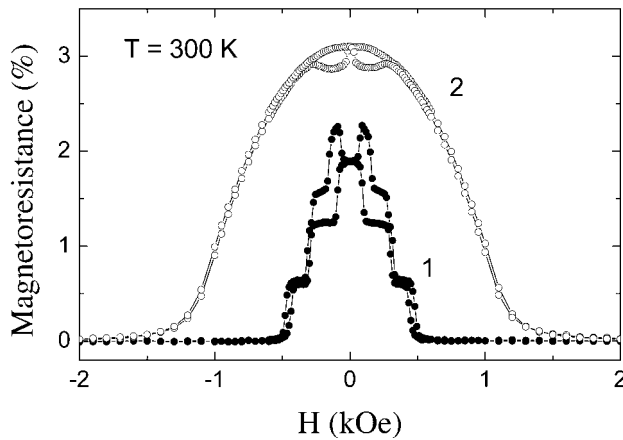


Fig. 5 Magnetoresistance $\Delta R/R_s$ for the sample 1. Magnetic field is applied along the easy axis (curve 1) and along the hard axis (curve 2) in the film plane.

Figures 4 and 5 demonstrate the qualitative difference of magnetization processes when the magnetic field is applied along the easy and hard axes. The easy axis hysteresis loops have pronounced steps, whereas the magnetization and magnetoresistance exhibit smooth field dependences for the hard axis. The any changes in magnetic ordering in the multilayer are followed by the modification of the magnetoresistance. This correlation has both the qualitative and quantitative character.

To analyse the stepwise GMR in connection with the change of a magnetic states, the descending branch of the hysteresis loop (a) and the corresponding branch of magnetoresistance (b) are presented in Fig. 6 in special units. The magnetization M is expressed in Fig. 6(a) in units of the magnetic moment M_0 of one Fe layer of this sample. The total magnetic moment of the superlattice changes discretely with steps proportional to $\Delta M = 2M_0$, with the exception of magnetic fields near the coercive field H_c . When the magnetic field changes from saturation field H_s to the $-H_s$, the superlattice goes through a number of

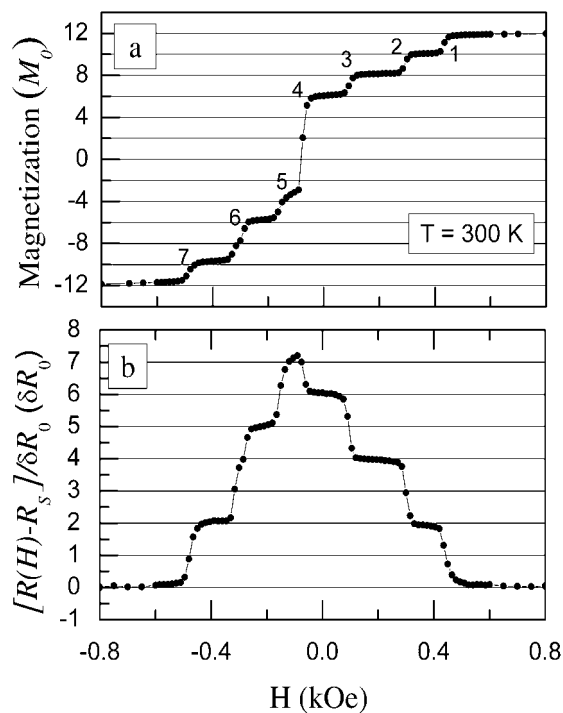


Fig. 6 Normalized descending branch of magnetization hysteresis loop and corresponding branch of GMR hysteresis loop for the sample 1. Magnetic field is applied along the easy axis in the film plane. The magnetization in Fig. 6(a) is expressed in units of the magnetic moment M_0 of a one Fe(85 Å) layer. The consecutive spin-flip transitions for the descending branch are indexed as shown. The magnetoresistance $\Delta R(H)/\delta R_0 = [R(H) - R_s]/\delta R_0$ is presented in Fig. 6(b) in units of δR_0 , where the δR_0 is the variation of the superlattice resistance due to one surface spin-flip transition.

collinear magnetic states corresponding to the following total magnetization (in units of M_0): $12M_0 \rightarrow 10M_0 \rightarrow 8M_0 \rightarrow 6M_0 \rightarrow (-3M_0) \rightarrow -6M_0 \rightarrow -10M_0 \rightarrow -12M_0$. For example, the step-anomaly (indexed as 1 in Fig. 6(a)) corresponds to the spin-flip transition, which means the flip of magnetic moment \mathbf{M}_i of the whole i -th magnetic layer. The total magnetization of the sample is decreased at this step by the value of $2M_0$ due to the compensation of two equal magnetic moments with opposite directions. The discrete change of the total magnetization demonstrates that: i) Fe layers have the equal thickness, and ii) the whole volumes of Fe layers are involved into spin-flip transitions, i.e. there are no magnetic domains inside of Fe layers between these transition when the collinear magnetic ordering exists in the multilayer.

Lets turn to the analysis of the magnetoresistance data. The normalized magnetoresistance $\Delta R(H)/\delta R_0$ is presented in Fig. 6(b). It is necessary to note that the typical electron free path in the Fe/Cr superlattice is $l \sim 10\div 100 \text{ \AA}$. The Fe/Cr superlattice under investigation has the superstructure period of $L \approx 100 \text{ \AA}$. The period is comparable or bigger than the electron free path, $L \geq l$. Hence, one can choose an elementary cell including the Cr spacer and two halves of the nearest magnetic layers. In this case ($L \geq l$) the electron scattering in different cells could be considered as independent. The change of the ordering of magnetic layers from ferromagnetic to antiferromagnetic in one sell leads to the magnetoresistance variation equal to δR_0 . One could separate the effects of the surface (external) spin-flip transition and the internal transition occurred inside the superlattice: the δR_0 step-change corresponds to a surface spin-flip transition, and the $2\delta R_0$ – to a spin-flip transition inside the superlattice. The flip of the magnetic moment \mathbf{M}_i located between two anti-parallel \mathbf{M}_{i+1} and \mathbf{M}_{i-1} moments will not change the superlattice resistance. The transition gives the equal resistance changes δR_0 but with opposite signs: $\Delta R = -\delta R_0 + \delta R_0 = 0$.

The comparative analysis of $M(H)$ and $\Delta R(H)/\delta R_0$ presented in Fig. 6 gives qualitative information about the sequence of spin-flip transitions. The $M(H)$ step anomalies indexed as 1, 2, 3 and 7 correspond to spin-flip transitions inside the superlattice ($\Delta M = 2M_0$, $\Delta R/\delta R_0 = 2\delta R_0$). The step number 6 in Fig. 6(a) corresponds to the sum of flips of one magnetic moment inside the superlattice and one external magnetic moments ($\Delta M = 4M_0$, $\Delta R/\delta R_0 = 3\delta R_0$). The complicate reconstruction of the magnetic order in the superlattice occurs in the magnetic fields near H_c , where the quantitative correlation between $M(H)$ and $\Delta R(H)/\delta R_0$ is not so clear. No transitions with the $\Delta M \neq 0$ and $\Delta R/\delta R_0 = 0$ simultaneously were detected. It means that magnetic moments involved into consecutive two spin-flip transitions do not belong to the adjacent layers in superlattice.

The investigation of the magnetic reversal processes demonstrates that each spin-flip transition is the first order phase transition followed by the irreversible magnetization and the minor hysteresis loop near step-anomalies on the $M(H)$ dependence (Fig. 7). The typical width of the plateau between two consecutive spin-flip transitions for the sample is $\Delta H = 200\div 300 \text{ Oe}$.

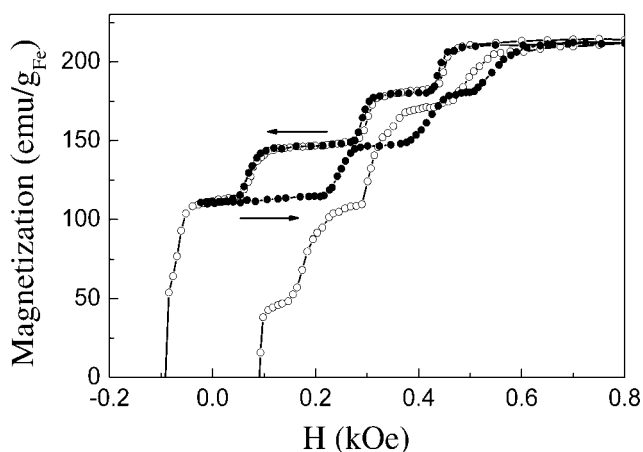


Fig. 7 Major (open circles) and minor (closed circles) hysteresis loops for the sample 1. Magnetic field is applied along the easy axis in the film plane.

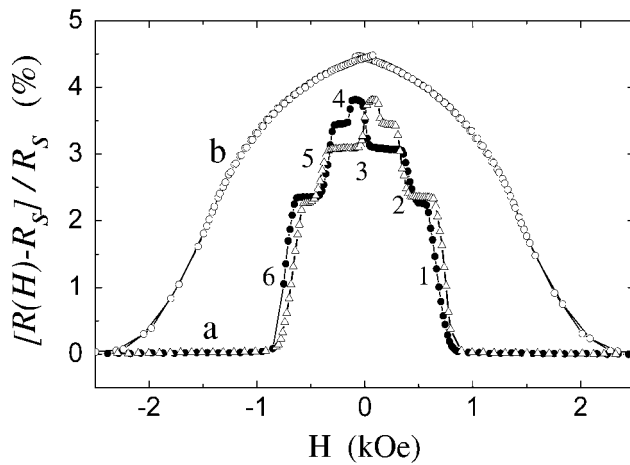


Fig. 8 Magnetoresistance $\Delta R/R_s$ for the sample 3 measured at room temperature. Magnetic field is applied along the easy axis (curve a) and along the hard axis (curve b) in the film plane. The solid points on the curve (a) correspond to the descending branch of the GMR hysteresis loop, and open triangles to the ascending branch. The consecutive spin-flip transitions for the descending branch are indexed as shown.

In the $(211)\text{MgO}/\text{Cr}(80\text{\AA})/[\text{Fe}(85\text{\AA})/\text{Cr}(12.4\text{\AA})]_{12}$ superlattice (sample 3) grown in the same conditions we reduced the nominal Cr layers thickness by the value of $\Delta t_{\text{Cr}} = 1.2 \text{ \AA}$. This Cr layers thickness reduction resulted in the more strong exchange coupling and the nearly twice higher saturation fields in comparison with $t_{\text{Cr}} = 13.6 \text{ \AA}$ superlattice, as shown in Fig. 8. The magnetoresistance in this sample have also the step-like anomalies when the magnetic field is applied along the easy axis in the film plane, but the sequence of spin-flip transitions is different. The analysis of $M(H)$ (the plot is not included in the paper) and $\Delta R(H)/\delta R_0$ for the descending branch of the hysteresis loop of the sample 3 have shown that: transitions indexed as 1 and 6 in Fig. 8 correspond to the flip of three internal magnetic moments, which are not neighbouring in the superlattice; transition 2 and 3 correspond to the consecutive flip of two not adjacent magnetic moments; the step 4 corresponds to the surface spin-flip transition; and transition 5 is the sum of flips of both one internal and one external (lowermost) magnetic moments. The sequence of spin-flip transitions differs from that revealed in the sample 1.

The experimental determination of the whole sequence of spin-flip transitions in the Fe/Cr superlattices with the large number ($n = 12$) of thick Fe layers exceeds the framework of the present paper.

4 Conclusions

We have grown the $(211)\text{MgO}/(210)[\text{Fe}/\text{Cr}]_{12}$ superlattices with the strong uniaxial in-plane anisotropy. The multi-stepwise magnetization and magnetoresistance behavior is found in the $[\text{Fe}(85 \text{ \AA})/\text{Cr}(t_{\text{Cr}})]_{12}$ superlattices with the $t_{\text{Cr}} = 13.6 \text{ \AA}$ and 12.4 \AA when the magnetic field is applied along the easy axis in the film plane. It is shown that the step-like anomalies are connecting with the magnetization reversal of individual Fe layers in macroscopic samples. The dependences $M(H)$ and $\Delta R(H)/R$ are smooth for the hard magnetization axis. The qualitative information about the sequence of spin-flip transitions in two samples is extracted from the comparative analysis of the magnetization and magnetoresistance. The high sensitivity of the spin-flip transitions sequence to a small variation of the Cr layers thickness in the superlattices is revealed.

Acknowledgements The research was supported by Grant of Russian Federation N 02.435.11.219, RFBR (Grants N 04-02-16464, N 05-02-08169-ofi-a), Programs of RAS “Quantum nanostructures” and “Quantum macrophysics”.

References

- [1] O. Hellwig, A. Berger, and E. Fullerton, Phys. Rev. Lett. **91**, 197203 (2003).
- [2] O. Hellwig, T. L. Kirk, J. B. Kortright, A. Berger, and E. E. Fullerton, Nature Mater. **2**, 112 (2003).
- [3] O. Hellwig, A. Berger, and E. E. Fullerton, J. Magn. Magn. Mater. **290/291**, 1 (2005).

- [4] T. Ślezak, W. Karaś, K. Krop, M. Kubik, D. Wilgocka-Ślezak, N. Spiridis, and J. Korecki, *J. Magn. Magn. Mater.* **240**, 362 (2002).
- [5] M. Żołądź, T. Slezak, D. Wilgocka-Slezak, N. Spiridis, J. Korecki, T. Stobiecki, and K. Röhl, *J. Magn. Magn. Mater.* **272-276**, 1253 (2004).
- [6] M. M. H. Willekens et al., in: *Magnetic Ultrathin Films: Multilayers and Surface, Interfaces and Characterization*, edited by B. T. Jonker et al., MRS Symp. Proc. No. 313 (Materials Research Society, Pittsburg, 1993), p. 129.
- [7] U. K. Röbber and A. N. Bogdanov, *J. Magn. Magn. Mater.* **269**, L287 (2004).
- [8] M. N. Babich, J. M. Broto, A. Fert, F. Nguyen Van Dau, and F. Petroff, *Phys. Rev. Lett.* **61**, 2472 (1988).
- [9] S. S. P. Parkin, N. More, and K. P. Roche, *Phys. Rev. Lett.* **64**, 2304 (1990).
- [10] E. E. Fullerton, M. J. Conover, J. E. Mattson, C. H. Sowers, and S. D. Bader, *Phys. Rev. B* **48**, 15755 (1993).
- [11] M. A. Tomaz and W. J. Antel, Jr., W. L. O'Brein, and G. R. Harp, *Phys. Rev. B* **55**, 3716 (1997).
- [12] R. W. Wang and D. L. Mills, *Phys. Rev. Lett.* **72**, 920 (1994).
- [13] S. G. E. te Velthuis, G. P. Felcher, J. S. Jiang, C. S. Nelson, A. Berger, and S. D. Bader, *Appl. Phys. Lett.* **75**(26), 4174 (1999).
- [14] J. S. Jiang, G. P. Felcher, A. Inomata, R. Goyette, C. Nelson, and S. D. Bader, *Phys. Rev. B* **61**, 9653 (2000).
- [15] S. G. E. te Velthuis, J. S. Jiang, and G. P. Felcher, *Appl. Phys. Lett.* **77**(14), 2222 (2000).
- [16] L. Lazar, J. S. Jiang, G. P. Felcher, A. Inomata, and S. D. Bader, *J. Magn. Magn. Mater.* **223**, 299 (2001).
- [17] P. B. Hirsch, A. Howie, R. B. Nicholson, D. W. Pashley, and M. J. Whelan, *Electron Microscopy of Thin Crystals* (Butterworths, London, 1965).